

## Numerical Study of an Interacting Rossby Wave and Barotropic Zonal Flow Near a Critical Level

J. E. GEISLER

*Rosenstiel School of Marine and Atmospheric Science, University of Miami, Coral Gables, Fla. 33124*

R. E. DICKINSON

*National Center for Atmospheric Research,<sup>1</sup> Boulder, Colo. 80303*

(Manuscript received 17 September 1973, in revised form 16 January 1974)

### ABSTRACT

This paper treats the initial value problem of a forced Rossby wave encountering a critical level in a barotropic zonal shear flow which can change in response to the wave momentum flux divergence. The main result of the calculation is that the shape of the zonal flow profile changes with time in such a way as to reduce the potential vorticity gradient ( $\beta - U_{yy}$ ) to zero at the critical level. For this configuration the wave is totally reflected at the critical level and in the absence of dissipation no longer interacts with the zonal flow. Details of the evolution toward the steady state depend on the ratio of two time scales, one a measure of the wave amplitude and the other representing the time it takes for the wave momentum flux to be concentrated in a well-defined critical layer.

The steady-state balance between wave and mean flow probably never occurs in the atmosphere because the time required to set it up is long compared to the expected time scale of natural variability of the zonal flow. More relevant to atmospheric flows is the fact that excursions of  $(\beta - U_{yy})$  to negative values during the approach to a steady state are attended by overreflection of the incident wave and a temporary reversal of the wave momentum flux. After the first of these excursions, occurring on a time scale comparable to that required to set up a critical layer, the zonal flow is never far from the final equilibrium profile.

### 1. Introduction

The tropical and extratropical atmosphere are to some degree coupled by lateral propagation of large-scale waves originating in middle latitudes. Linear theory (e.g., Charney, 1969) applied to a single wave in a zonal flow shows that no propagation can take place in a region where the zonal flow is more easterly than the phase speed of the wave. The surface which separates this region from the one further north where the wave propagates laterally is the *critical level* for the wave. On this surface the phase speed of the wave matches the zonal flow and the steady linear wave equation is singular. Here the wave interacts with the zonal flow, coupling the zonally averaged motion in the tropics to sources of middle wave motion.

The assumption that the vertical shear of the zonal wind can be neglected, permitting separability of the wave equation, allows considerable simplification in the formulation of a model for studying the interaction of a laterally propagating large-scale wave with the zonal flow at a critical level. For in this circumstance, following an argument first used by Charney (1963), one can show that in low latitudes the equation govern-

ing large-scale waves with a vertical structure typical of middle latitudes reduces to the nondivergent, barotropic vorticity equation. Accordingly, the model considered in this paper is a homogeneous fluid with a rigid lid situated on a  $\beta$ -plane.

The case of a steady single wave propagating in a barotropic fluid from a source to a critical level in a linear shear flow was described by Dickinson (1968). The solution consists of a wave which originates at the source and is completely absorbed at the critical level, where the energy flux jumps to zero. The momentum flux is constant, directed from the critical level to the source and also jumps to zero across the critical level. The steady-wave solution is not entirely satisfactory because of the existence of a logarithmic singularity in the zonal component of the wave velocity field which violates the linearization. To establish a time scale for the breakdown of the linearization, Dickinson (1970) solved the initial value problem in which the wave field developed with time from a switch-on source while the linear shear flow was held constant in time. This analysis showed that a concentrated momentum flux divergence occurs over a *critical layer* whose thickness decreases with time. The time scale on which the logarithmic singularity and the narrowing of the critical layer to a critical level occur was shown to be long

<sup>1</sup>The National Center for Atmospheric Research is sponsored by the National Science Foundation.

compared to the expected time scale for variability of atmospheric zonal flows. It was concluded that the flux divergence that occurs as a delta function in the steady-wave solution would occur in the atmosphere distributed across a critical layer at least a few hundred kilometers in latitudinal extent.

This initial value problem was again solved by Bennett and Young (1971) in the course of a numerical investigation of waves in a simple model tropics forced by middle latitude sources. The time scale on which the steady wave could be set up was estimated from the appearance of the numerical solutions and from a group velocity argument applied to a WKB description of propagation between source and critical level. Since the WKB approximation is not valid near a critical level, the time scale obtained by this argument is not necessarily the same as the time scale on which the development of a critical layer occurs. The distinction between these two time scales is clarified by a calculation described in Section 3.

The purpose of the present study is to treat the initial value problem of the wave and the zonal flow as an interacting system. After the switch-on of a wave source far to the north of a critical level, wave momentum flux divergence becomes more and more concentrated in a critical layer whose thickness decreases with time. Positive momentum is removed from the zonal flow in this layer, forming a ledge in the profile and drawing the critical level closer to the wave source. The zonal flow vorticity gradient  $U_{yy}$  increases in the layer as the ledge gets sharper and enters the wave equation in the coefficient  $(\beta - U_{yy})$ . When this becomes negative, the wave momentum flux divergence changes sign, positive momentum flows into the critical layer, and the ledge begins to fill. The calculation to be described shows that the interaction is one of negative feedback, and after a number of oscillations  $(\beta - U_{yy})$  is reduced to zero at the critical level. The incident wave is then totally reflected there, giving a standing wave in the domain between source and critical level that transports no momentum and has no further influence on the zonal flow.

Some net positive momentum is removed from the zonal flow over the time between the initial instant and the final steady state. How much depends not only on the amplitude of the wave but also on the time it takes to set up a critical layer. The dependence of this time on the shear in the zonal flow and the wavenumber of the disturbance is considered in Section 3. There we describe solutions of the initial value problem in a fixed zonal flow that extend the analysis of Dickinson (1970) to shear flows with curvature and over a wider region of parameter space. The coupled wave and zonal flow solutions are presented in Section 4.

**2. Formulation**

We consider quasi-geostrophic, nondivergent wave motion forced by a localized source of wave vorticity

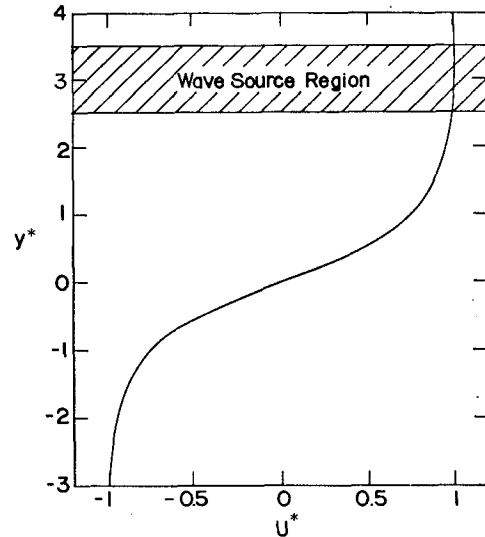


FIG. 1. Hyperbolic tangent zonal flow profile in dimensionless units. Position of wave source shown by hatching.

switched on at  $t=0$  and maintained constant. The linearized vorticity equation for the disturbance on a zonal flow  $U(y,t)$  is then

$$\left(\frac{\partial}{\partial t} + U \frac{\partial}{\partial x}\right)(\Psi_{xx} + \Psi_{yy}) + (\beta - U_{yy})\Psi_x = S. \tag{1}$$

Here  $x, y$  are coordinates positive to east and north on a  $\beta$ -plane and  $u, v$  the corresponding components of wave velocity, related to the wave streamfunction  $\Psi$  as

$$u = -\frac{\partial \Psi}{\partial y}, \quad v = \frac{\partial \Psi}{\partial x}. \tag{2}$$

The equation governing the zonal flow is

$$\frac{\partial U}{\partial t} = -\frac{\partial}{\partial y}(\overline{uv}), \tag{3}$$

where the overbar denotes a zonal average.

The geometry for the problem is illustrated in Fig. 1. For the zonal flow at the initial time we adopt the hyperbolic tangent profile

$$U = U_m \tanh(y/L), \tag{4}$$

where  $U_m$  and  $L$  are scales to be chosen. The critical level for a stationary wave (zero zonal phase velocity) will lie at the center of the profile. This position can be changed by adding a constant to (4), thus shifting the profile to the right or to the left. The stationary wave vorticity source is taken to be

$$S(x,y) = \text{Re}[iG(y) \exp(ikx)], \tag{5}$$

where  $k$  is the zonal wavenumber and  $G(y)$  is a narrow Gaussian situated north of the shear zone. Because of

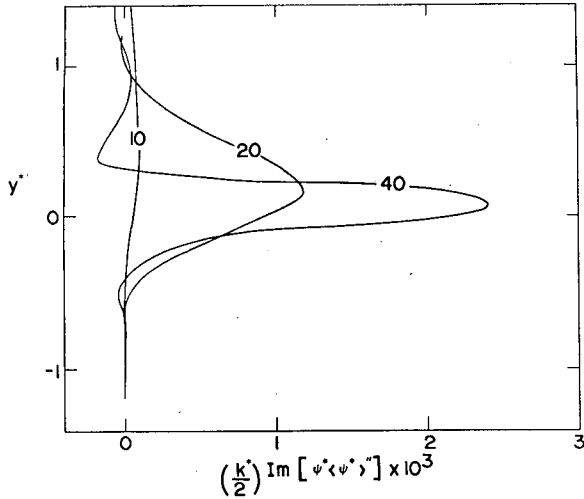


FIG. 2. Dimensionless wave momentum flux divergence at successive days after the switch-on of wave source. Zonal flow is fixed with time and critical level is at  $y^*=0$ .

the assumed structure (5), the wave field will have the structure

$$\Psi(x, y, t) = \text{Re}[\psi(y, t) \exp(ikx)]. \tag{6}$$

Nondimensional (asterisked) quantities are introduced as follows:

$$\left. \begin{aligned} y^* &= \frac{y}{L}, & k^* &= kL, & t^* &= \frac{U_m t}{L}, & U^* &= \frac{U}{U_m} \\ \beta^* &= \frac{\beta L^2}{U_m}, & \psi^* &= \frac{\psi}{U_m L}, & G^* &= \frac{L^2}{U_m^2} G \end{aligned} \right\} \tag{7}$$

With appropriate substitutions and using (5) and (6), Eq. (1) becomes

$$\left[ \left( \frac{\partial}{\partial t^*} + U^* i k^* \right) \left( \frac{\partial^2}{\partial y^{*2}} - k^{*2} \right) + i k^* (\beta^* - U^{*''}) \right] \psi^* = i G^*, \tag{8}$$

where a prime denotes differentiation with respect to the dimensionless variable  $y^*$ . After the average in the zonal direction is taken, Eq. (3) becomes

$$\frac{\partial U^*}{\partial t^*} = -\frac{k^*}{2} \text{Im}(\psi^* \langle \psi^* \rangle'), \tag{9}$$

the symbol  $\langle \rangle$  denoting the complex conjugate, and  $\text{Im}$  the imaginary part of.

In the case where the zonal flow  $U^*$  is held constant in time, Eq. (8) may be integrated forward in time from the initial condition of  $\psi^*=0$  using an implicit scheme, as done previously by Bennett and Young (1971). When the zonal flow is evolved in time along with the wave the use of an implicit scheme for (8)

leads to computational instability. A stable solution was obtained by using the scheme of Matsuno (1966) with a very small time step. The grid point spacing used in all calculations is  $\Delta y^*=0.06$ . A discussion of the means used to simulate a radiation boundary condition is contained in an appendix.

### 3. Solutions in a fixed zonal flow

In this section we describe solutions of Eq. (8) with the zonal flow independent of time and given by the hyperbolic tangent profile (4). The corresponding initial value problem for a zonal flow varying linearly with  $y$  was treated in Dickinson (1970). There space and time variables were non-dimensionalized by length and time scales (denoted by  $Y_c$  and  $T_c$  for the present paper) defined as

$$Y_c = U'/\beta, \quad T_c = \beta/(U'^2 k), \tag{10}$$

where  $U'$  is the constant shear in the zonal flow. For dimensionless time of order unity or larger the wave momentum flux divergence was found to be concentrated in a critical layer of dimensionless width of order  $(\text{time})^{-2}$ . We establish here that these scales apply locally to a critical level located at any point on the hyperbolic tangent zonal flow profile. In terms of variables defined by (7) the scales are given by

$$\left. \begin{aligned} Y_c^* &= U^{*'} / (\beta^* - U^{*''}) \\ T_c^* &= (\beta^* - U^{*''}) / [(U^{*'})^2 k^*] \end{aligned} \right\} \tag{11}$$

where the prime denotes differentiation with respect to the dimensionless variable  $y^*$ .

Fig. 2 shows the evolution with time of the wave momentum flux divergence when the critical level is situated at the center of the profile, at which point  $U^{*'}=1$  and  $U^{*''}=0$ . For the case shown  $U_m/L=1 \times 10^{-5} \text{ sec}^{-1}$ ,  $\beta=2 \times 10^{-13} \text{ sec}^{-1}$ ,  $L=10^3 \text{ km}$  and  $k=4 \times 10^{-9} \text{ cm}^{-1}$ , corresponding to a zonal wavenumber 2. This choice gives  $Y_c^*=0.5$ ,  $T_c^*=5$  and  $T_c \approx 6$  days. A critical layer

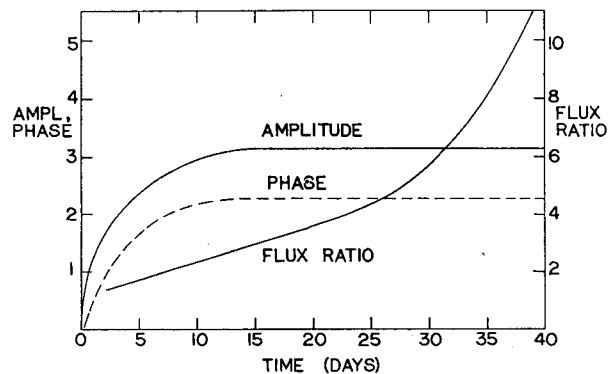


FIG. 3. Time scales in the development of a critical layer in a fixed zonal flow for  $T_c \approx 6$  days. Behavior of amplitude and phase of wave indicate apparent steady state in wave field after about 15 days. Ratio of momentum flux across critical level continues to evolve beyond this time.

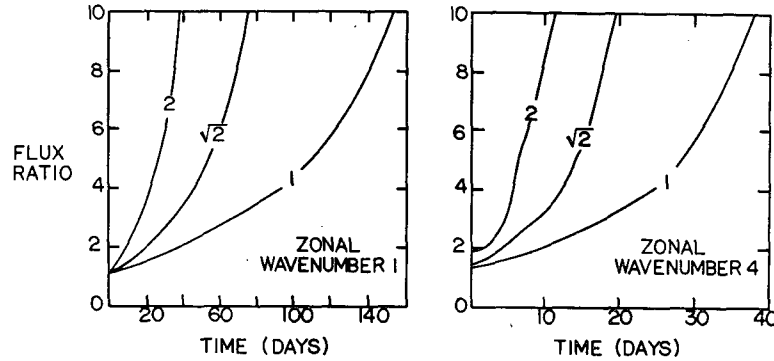


FIG. 4. Ratio of momentum flux across critical level versus time. Zonal flow profile is fixed in time. Curves are labelled by shear (units of  $10^{-5} \text{ sec}^{-1}$ ) at the critical level, located at  $y^*=0$ .

with dimensionless width of order unity forms somewhere between 10 and 20 days. Between 20 and 40 days, the width of the layer appears to decrease by a factor of 4 approximately. The ratio of momentum flux at  $y^*=0.12$  to that at  $y^*=-0.12$  (2 grid point spaces to each side of the critical level) is shown in Fig. 3. Also shown is the evolution of wave amplitude and phase at the critical level. This illustrates that the critical layer continues to develop beyond the time required for the wave field to appear to have reached a steady state. The case for a linear profile with the same parameters (shear =  $10^{-5} \text{ sec}^{-1}$  and wavenumber 2) was calculated by Bennett and Young (1971) who found that the wave appeared to reach a steady state in about 15 days, in agreement with the result shown in Fig. 3.

In the numerical solutions the momentum flux ratio at two points close to, but on either side of, the critical level continues to increase with time until the flux divergence peak narrows to a width comparable to the grid point spacing, at which time the wave begins to reflect. In the case under discussion here, this occurs when the ratio is about 25. An arbitrary, but small, amount of linear drag can be put into the problem to bring the solution to a steady state before this occurs, in effect smearing out the critical level over several grid points. As an alternative we arbitrarily define the time required for a steady solution to be set up as the time required for the flux ratio at two specified points either side of the critical level to reach 10. This will be the definition of the term "time required to set up a critical layer" as used in this paper. We have run a large number of cases to find that the dependence of this time on  $\beta$ ,  $U'$  and  $k$  is essentially that for the time scale  $T_c$  given in (10) and (11), wherever the critical level may be on the zonal wind profile. Fig. 4 shows this result for three values of shear and two wavenumbers when the critical level is situated at the middle of the hyperbolic tangent profile. For wavenumbers higher than 4 the wave is evanescent away from the source. When the critical level is situated at another point on the

profile,  $U'' \neq 0$  so that  $V_c^*$  will change, and this necessitates a different choice for the two points where the flux ratio is computed in order that the results be comparable with those for the case where the critical level is at the center of the profile. These results are not shown here.

This calculation establishes that the time required to set up a critical layer in a hyperbolic tangent shear flow depends on the local shear at the critical level and not on the overall shape of the profile. In particular, the dependence of this time constant on the parameters of the problem is essentially that for the time constant  $T_c$  obtained in the linear shear flow problem treated in Dickinson (1970). From the numerical results presented here we conclude that its value is  $\lesssim 10T_c$ .

#### 4. Solutions in an evolving zonal flow

In this calculation the zonal flow responds to the wave momentum flux divergence. The wave equation (8) and the zonal flow equation (9) are solved as a coupled pair. For a representative case we let the critical level be situated in the middle of the hyperbolic tangent profile and consider a zonal wavenumber 5 disturbance switched on at the initial time, choosing for dimensional value of shear at the critical level  $U_m/L = 2 \times 10^{-5} \text{ sec}^{-1}$  and for the characteristic width of the hyperbolic tangent shear zone  $L = 10^3 \text{ km}$ . This choice of parameters gives  $T_c = 0.6 \text{ day}$ . Changes in the zonal flow pattern with time are followed in Fig. 5. At 9 days a ledge in the zonal flow has formed in response to the wave momentum flux divergence concentrated in a fully developed critical layer. The curvature associated with the ledge results in a region of negative ( $\beta^* - U''$ ) [hereafter referred to as  $\beta$  effective] near the critical level. Subsequent interaction of the wave with the zonal flow profile irons out this ledge in such a way as to reduce  $\beta$  effective to zero at the critical level. Inspection of the phase and amplitude behavior of the evolving wave (not shown) confirms that reflection of the wave at the critical level becomes total as  $\beta$  effective settles down to zero. The resulting

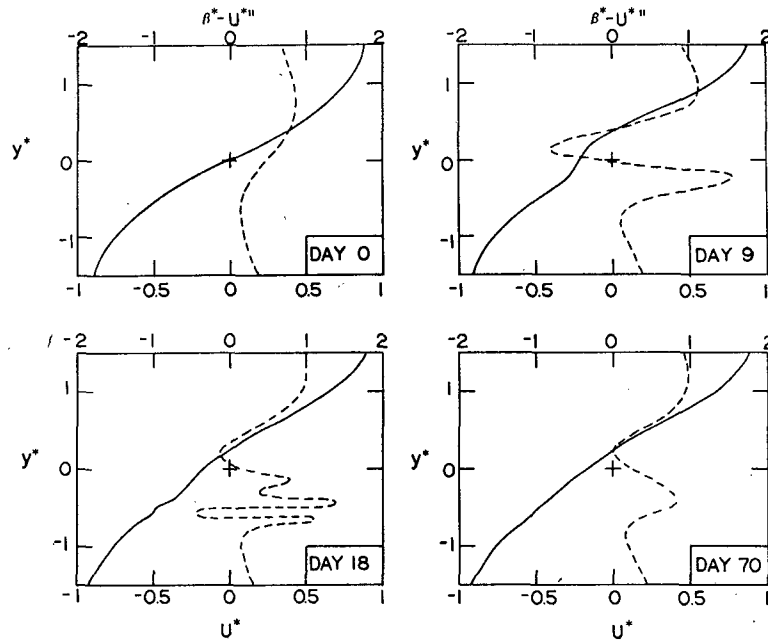


FIG. 5. Details the evolution of zonal flow (solid curve) and  $\beta$  effective (dashed curve) as it interacts with wave incident from the source at  $y^*=3$ . Parameters for this case are  $U_m=20 \text{ m sec}^{-1}$ ,  $L=10^6 \text{ km}$ ,  $\beta=2 \times 10^{-13} \text{ cm}^{-1} \text{ sec}^{-1}$  and zonal wave-number 5.

steady state is for all practical purpose realized in the present example in about 70 days.

Further discussion of the behavior of this solution can be made with reference to Fig. 6, where the continuous line is the wave momentum flux at  $y^*=2.5$ , just to the south of the wave source. After the initial instant, as the critical-layer develops, the wave is extracting positive zonal momentum from the zonal flow. Around 9 days,  $\beta$  effective evolves through a zero near the instantaneous critical level and becomes

negative. The positive flux divergence peak collapses and is replaced by a negative flux divergence peak. Positive momentum is then brought back into the region across  $y^*=2.5$ . As Fig. 6 shows, this cycling of momentum in and out of the region continues for some time as a steady state is gradually approached. This sequence of events is an example of "overreflection" as defined and as described for a steady wave solution by Dickinson and Clare (1973). When a steady wave is incident from the north, whatever the sign of  $\beta$  effective at the critical level, there is a positive flux of momentum on the northern side and no momentum flux on the southern side where the wave is evanescent, hence there must be momentum flux divergence at the critical level. Now if  $\beta$  effective is negative at the critical level, there is northward (down gradient) transport of potential vorticity there, hence net momentum flux convergence. This net convergence requires the presence in the solution of a reflected wave with amplitude larger than the incident wave. Such overreflection comes at the expense of the zonal flow and the present calculation shows that it acts to restore the zonal flow configuration to one that leads to ordinary total reflection of the incident wave.

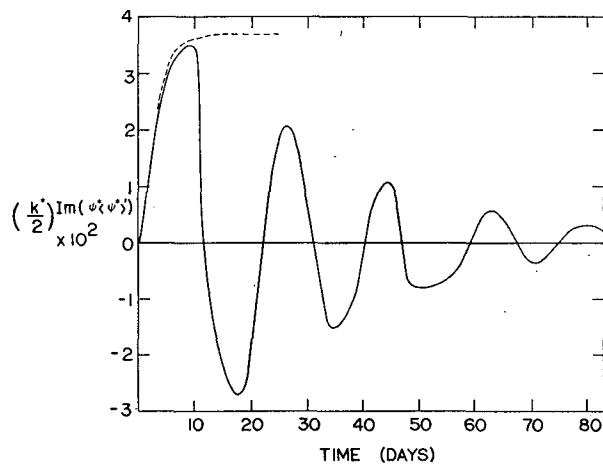


FIG. 6. Dimensionless wave momentum flux (solid curve) at a point just to the south of the wave source for the interacting case in Fig. 5. Flux when zonal flow profile is held fixed in time is shown by dashed curve.

We present next numerical solutions intended to explore the parameter space of the problem. The important parameters are the amplitude of the wave and the time it takes to set up a critical layer. As shown in Section 3, the latter is proportional to the time scale  $T_c$ . If the amplitude of the wave is very large, or if  $T_c$  is very long, then momentum will be taken from the

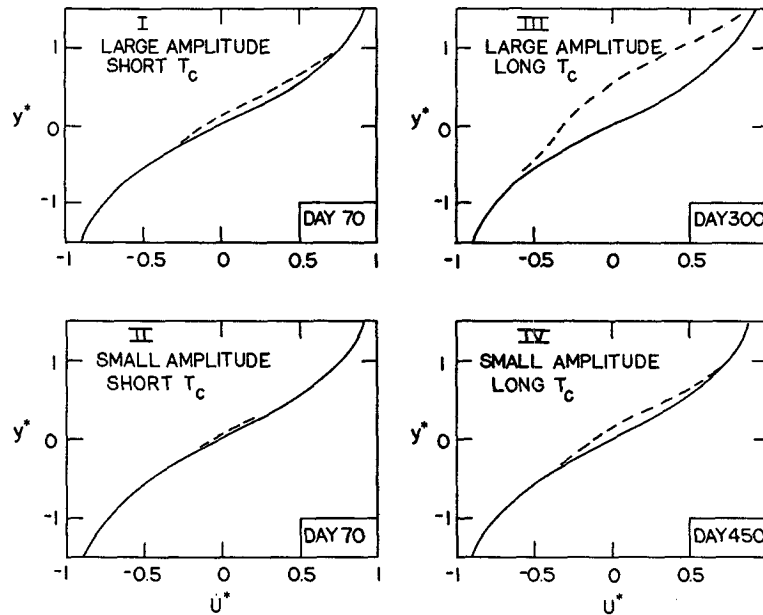


FIG. 7. Initial (solid) and final (dashed) zonal flow profiles for four cases defined by values in Table 1 for  $U_m$ ,  $L$ , wavenumber (specifying  $T_c$ ) and  $F^*$  (a function of wave amplitude).

zonal flow over a region wide compared to the thickness of a fully developed critical level. A relatively large amount of momentum will have to be removed before the profile curvature is sufficient to produce overreflection. The interaction between wave and zonal flow is occurring over such a broad region that the concept of critical level absorption is not useful in describing the coupling. For a wave of very small amplitude or for very short  $T_c$ , a critical layer will develop before there is any overreflection. A relatively small amount of zonal momentum will be removed from a narrow range of latitude, but this deficit is subsequently spread over some wider range in order that  $\beta$  effective be reduced to zero at the critical level.

It is convenient to characterize the amplitude of the wave by a time constant  $T_z$  which is the time required for a constant wave momentum flux  $F$  to extract a given amount of momentum from the zonal flow. From (7) we nondimensionalize Eq. (3) governing zonal changes to obtain

$$\frac{\partial U^*}{\partial t^*} = -\frac{\partial F^*}{\partial y^*}, \tag{12}$$

where  $F^* = F/U_m^2$ . Integration over time from zero to  $T_z^*$  and over latitude to some  $y^*$  near the source of the constant flux gives

$$T_z^* = (F^*)^{-1} \int_{-\infty}^{y^*} \Delta u^* dy^*. \tag{13}$$

We arbitrarily set the value of the integral to 0.1, which is approximately the area between the initial

and final curves in Fig. 5, and maintain this value for all cases described below. To complete the definition of  $T_z^*$  we take  $F^*$  to be the maximum northward flux at a point just to the south of the wave source region. For example, for the case treated in detail earlier in this section, we would define  $T_z^*$  using the flux at the first peak on the continuous  $T_z$  curve in Fig. 6. This is about equal to the flux that would be carried by a wave of the same amplitude in a fixed zonal flow, which has been plotted with a dashed curve in Fig. 6.

Parameters for four separate solutions of the coupled initial value problem are summarized in Table 1. Change in the zonal flow profile brought about by the wave in each of these cases is seen in Fig. 7. Initial profiles, the same in all cases, are represented by continuous lines. Final profiles are represented by dashed lines. The cases on the left have reached a steady state,

TABLE 1. Zonal flow profile scales ( $U_m$  and  $L$ ) and initial shear [ $U'(0)$ ] at center of profile for cases shown in Fig. 7. Incident wave is characterized by the zonal wavenumber and the maximum dimensionless momentum flux  $F^*$ .

	Case			
	I	II	III	IV
$U_m$ (m sec <sup>-1</sup> )	20	20	5	5
$L$ (km)	1000	1000	500	500
$U'(0)$ (sec <sup>-1</sup> )	$2 \times 10^{-5}$	$2 \times 10^{-5}$	$10^{-5}$	$10^{-5}$
Wavenumber	5	5	1	1
$F^*$	$2 \times 10^{-2}$	$2 \times 10^{-3}$	$2 \times 10^{-2}$	$2 \times 10^{-3}$
$F$ (m <sup>2</sup> sec <sup>-2</sup> )	8	0.8	0.5	0.05
$T_z$ (days)	3	30	6	60
$T_c$ (days)	0.6	0.6	12	12

and those on the right are very close to a steady state. Times required to attain a steady state are rather long compared to the time scale of seasonal variability for atmospheric zonal flows. On the other hand, from the case where the time evolution of the solution was followed (see Fig. 5), it is clear that much of the time required for the steady state to be reached is consumed in small changes of profile curvature, with very little change in the appearance of the profile. This feature of the evolution of the zonal flow toward a steady state is common to all of the cases shown in Fig. 7. We have examined the zonal flow profiles at the time when  $\beta$  effective first passes through zero and found them to be very close to the steady-state profiles shown there. In particular, the area between the profile at that time and the initial profile cannot be distinguished from the area between curves in Fig. 7. We conclude that most of the momentum extracted from the zonal flow is accomplished in the time it takes for  $\beta$  effective to first go to zero. In all four cases this time is comparable with but always less than  $10 T_c$ , which we earlier established as a measure of the time required to set up a critical layer in a time invariant zonal flow.

With reference to Fig. 7, the interaction between wave and mean flow in the four cases may be described as follows:

#### CASE I, $T_z \approx 10T_c$ .

This case is similar to that followed in detail earlier in this section. A critical layer is set up, creating a ledge in the zonal flow profile which is subsequently smeared out until  $\beta$  effective settles down to zero at the critical level.

#### CASE II, $T_z \gg 10T_c$ .

A very concentrated flux divergence peak has time to develop. This produces a small ledge and very little change elsewhere in the profile. Subsequent adjustment to a steady state redistributes the small momentum deficit over a rather wide interval, producing a final profile not much different from the original one.

#### CASE III, $T_z \ll 10T_c$ .

The amplitude of the wave is so large that the zonal flow is altered over a wide region well before a critical layer develops. There is a very large shift in the position of the critical level. Ultimately  $\beta$  effective is reduced to zero over a broad region centered there and the wave is totally reflected.

#### CASE IV, $T_z \approx 10T_c$ .

In this case it takes a long time for a critical layer to develop, but the amplitude of the wave is sufficiently small that the zonal flow profile is slow to change also. The evolving solution qualitatively resembles that in Case I on a much longer time scale.

Because of the relatively long  $T_z$  in Case II the net amount of momentum removed from the zonal flow is much less than that which was arbitrarily specified in the definition of  $T_z$ . From this case we can see that in the limit of very small  $T_c$  (high shear or zonal wavenumber) overreflection prevents any interaction between wave and mean flow. Conversion of the maximum wave momentum flux in the four cases to dimensional units is given in Table 1. The observed eddy momentum flux in the subtropics is of the order of  $10 \text{ m}^2 \text{ sec}^{-2}$  so that with the exception of Case I the assumed wave amplitudes are rather small. If these are increased,  $T_z$  is decreased. Then Case IV looks more like III and II looks more like I.

Wave amplitudes have been chosen to give maximum momentum fluxes such that the ratio  $T_z/T_c$  is very nearly the same in Cases I and IV. From the appearance of the final profiles for these cases in Fig. 7, we conclude that if the ratio of these times is held fixed, the change in the zonal flow pattern looks the same when the profiles have been scaled appropriately. If dimensional variables were plotted, the area between curves in Case IV would be eight times smaller than the area in Case I, following from the fact (see Table 1) that velocity and length scales are respectively four times and twice as small.

## 5. Discussion

According to the results of this study, a stable feedback accompanies critical layer absorption of a Rossby wave in a barotropic zonal flow. Creation of a ledge in the zonal flow profile proceeds only as far as the stage where curvature of the ledge forces  $\beta$  effective to go negative. Overreflection of the incident wave then reverses the sign of the wave momentum transport and the ledge fills until  $\beta$  effective is positive again. The process continues as a damped oscillation until a steady state is reached in which the incident wave is totally reflected at the critical level. This behavior is very much different from that of vertically propagating internal gravity waves encountering a critical level in a vertical shear flow, treated as a coupled wave and mean flow initial value problem by Jones and Houghton (1971). They showed that momentum transferred to the mean flow leads immediately to the formation of a step in the mean flow profile. The step remains fixed at the location of the critical level and increases in strength with time, with no indication of an approach to a steady state.

Interaction of *vertically* propagating Rossby waves with zonal flows was treated in a time-dependent calculation by Matsuno (1971) and applied there to model sudden stratospheric warmings. The wave is switched on at the lower boundary and removes westerly momentum at very high levels in the atmosphere where the density is low, creating a region of easterlies there. Subsequent interaction is localized in a developing critical layer at the base of the easterly regime. The

critical level is drawn downward toward the wave source at a decreasing rate in an approach to a steady state which was attributed by Matsuno (1971) to the increase of density as the critical level digs deeper down into the atmosphere. On the basis of our experience with the calculation described here, we would conjecture that a steady state in the vertical propagation case is approached because the zonal flow adjusts to give  $\beta$  effective equal to zero and reflects the incident wave. How the zonal flow accomplishes this cannot be inferred from the present calculation, since both first and second derivatives of zonal flow contribute to the potential vorticity gradient in the vertical problem.

Vertical and horizontal coupling through interaction of planetary-scale waves with the zonal flow should be included in general circulation models. Results obtained here can be used to infer conditions under which present day models can be expected to give a reasonable simulation of horizontal coupling by this mechanism. If the time scale required to change the zonal flow ( $T_z$ ) is much less than the time to set up a critical layer ( $\sim 10T_c$ ), then the interaction will take place over a region of width order unity in the dimensionless latitude coordinate, typically 500 km or more. Case III is an example. At the other extreme is Case II, where  $T_z \gg 10T_c$ . Here the interaction with the zonal flow takes place in a fully developed critical layer whose width is order  $10^{-1}$  of the dimensionless latitude coordinate. Such a distance scale cannot be resolved with the grid point spacing used in present general circulation models. However, the present calculation shows that because of the early onset of overreflection in this case, there is very little net transfer of momentum to the zonal flow anyway.

The fact that the critical layer interaction process in a barotropic fluid acts to reduce  $\beta$  effective to zero has some implications for both observational and theoretical studies. The time scale to reach this steady-state condition is so long that it is not likely that the zonal flow will remain fixed, but the tendency to minimize  $\beta$  effective could show up as a statistical effect of repeated critical level absorption events. Rather low values of  $\beta$  effective seem to characterize the summer average circulation in the tropical upper troposphere as summarized by Krishnamurti (1971). Fig. 2.5 of that paper gives contours of seasonal mean relative vorticity from which an estimate of the zonally-averaged vorticity gradient can be made. There is a broad region between the equator and 15N where  $U_{\text{zonal}}$  is within a factor of 2 of  $\beta$  and of the right sign to give  $\beta$  effective  $\approx 0$ . Throughout the region, the zonally-averaged flow is easterly, and critical levels exist only for waves propagating toward the west with phase speeds up to 10 m  $\text{sec}^{-1}$ . Such waves do indeed show up in the data (Krishnamurti, 1971), but their source is not clear. Statistical models of atmospheric circulation which incorporate lateral coupling by large-scale waves may have to take into account the tendency to minimize  $\beta$

effective. For example, in the model study by Mak (1969) of wave motion in the tropics consequent to stochastic boundary forcing, the zonal flow was held constant in time. Our calculation suggests that if the wave field in such a model were allowed to change the zonal flow, the result would be a statistically stationary zonal wind profile that would reflect back into middle latitudes the energy in waves that see critical levels.

The barotropic, nondivergent model that has been used here gives insight into a mechanism that must operate when a large-scale Rossby wave originating in middle latitudes encounters a critical level in lower latitudes. How well the model applies directly to the atmosphere is difficult to say. In a basic flow with no vertical shear the latitudinal dependence of the amplitude of each Fourier component of the wave's vertical structure is governed by a divergent, barotropic vorticity equation. As the equator is approached, the divergence term goes to zero and for a given latitude is smaller the smaller the vertical wavenumber of the Fourier component. It is in this sense that a barotropic vorticity equation governs the disturbance. Our model is strictly valid only if the critical level is right on the equator and for some distance away from it provided the vertical wavelength of the wave coming from middle latitudes is large.

Our model is quasi-nonlinear in that it allows for interaction between the wave and the zonal flow but does not allow the wave to interact with itself. The interaction of the wave with the zonal flow is correctly described by the model whether or not the wave's velocity field is small compared to the zonal flow. Neglect of the self-interaction, on the other hand, is strictly valid only if the wave amplitude is infinitesimal. The interaction of one zonal wavenumber with other zonal wavenumbers is another nonlinearity that is not described here since only one wavenumber is present in the calculation.

In no region of parameter space that we explored did the wave experience any sort of sustained growth at the expense of the zonal flow that could be usefully described as barotropic instability. Exponential growth of wave amplitude to very large values occurred only when the program was modified to decouple the zonal flow from the wave after  $\beta$  effective went negative. From this we conclude that the barotropic instability growth rate at the wavenumber of the forced wave is comparable to or less than the inverse of the time scale on which  $\beta$  effective is changed by the wave zonal flow interaction. Barotropic instability could play a role in a modified version of this model in which we continue to force only at a single wavenumber but carry other wavenumbers along in the calculation with the expectation that power will appear in these wavenumbers via barotropic instability whenever  $\beta$  effective of the zonal flow is driven negative by the forced wave. If the growth rate in some part of the spectrum of these additional wavenumbers were much larger than



the growth rate of barotropic instability at the forced wavenumber and these were allowed to modify the zonal flow, there is the possibility that the zonal flow might evolve differently. Some indication that this situation cannot be realized for moderately wide shear zones and planetary-scale forcing can be inferred from the barotropic instability growth rates tabulated in Dickinson and Clare (1973). From their Table 1 for  $\beta=0$  (largest negative peak value of  $\beta$  effective) maximum growth rates occur in the vicinity of nondimensional  $k^2=0.2$  and decrease rapidly going toward higher wavenumbers. For a shear zone width  $L=1000$  km this is approximately wavenumber 2.

A further shortcoming of our model lies in the treatment of the zonal flow. This is assumed to respond directly to the momentum flux divergence, as appropriate to a nondivergent, barotropic fluid. The response of atmospheric zonal flows is much more complicated [see, for example, the discussion in Dickinson (1971)]. Assume for the purpose of discussion that a wave with large amplitude in the upper troposphere is reasonably described by the barotropic vorticity equation and propagates equatorward to encounter a critical level at some latitude. Large momentum divergence aloft cannot change just the zonal flow there without producing a departure from geostrophic thermal wind balance and so will force a meridional overturning, changing the temperature field while Coriolis torques redistribute zonal momentum in the vertical. The resulting geostrophically balanced configuration is characterized by a distribution of potential vorticity dictated by the rearrangement of potential vorticity by the wave. Also, there are independent factors controlling the zonal flow variation. Thus, during the time required to set up a critical layer, changes may occur in the zonally averaged release of latent heat in the ITCZ or in the latitudinal variation of zonally averaged radiative cooling. Accompanying changes in the meridional overturning would then occur in the zonal flow through the action of Coriolis torques. Finally, as an additional mechanism not included here, dissipative process will tend to remove a concentration of zonal momentum in the vicinity of a critical level.

*Acknowledgments.* Most of the numerical work in the course of this investigation was done at the Computing Facility of the National Center for Atmospheric Research. The authors wish to thank Mr. George Ward, a student in the summer program in computing at the Center, for his help with the calculations. The research time of Dr. Geisler was supported by the National Science Foundation under Grant GA 34944.

#### APPENDIX

##### Boundary Effects

Fig. 8 shows an example of the complete zonal flow profile used in this study. The wave was allowed to

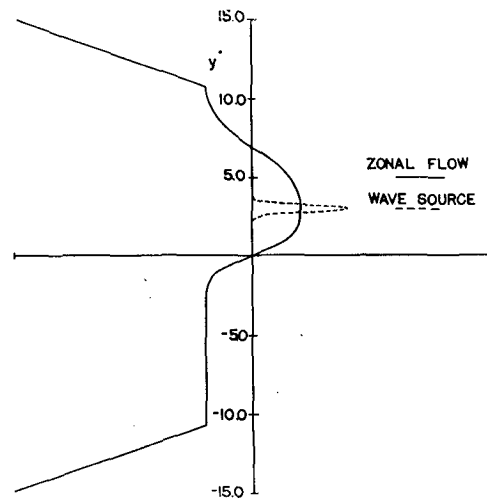


FIG. 8. The zonal flow configuration used to minimize boundary effects.

interact with the zonal flow only in the region to the south of the wave source in  $y^* \leq 2.5$ . Another hyperbolic tangent zonal flow profile has been joined on in the center of the wave source and extends northward from there to give a critical level that absorbs the wave coming out of the northern side of the source region. As the wave does not interact with the zonal flow on this side of the source, this critical level remains fixed. Inspection of the numerical solutions showed that for all zonal wavenumbers the steady wave north of the source is evanescent on the other side of this level and is down at least two orders of magnitude at the boundary located at  $y^*=15$ . A similar attenuation takes place between the critical level south of the source and the southern boundary at  $y^*=-15$ .

When the source is switched on, a spectrum of transient normal modes is excited. These show up as oscillations in the solutions which are not very effectively damped even by the Matsuno time scheme. Experiments with turning on the source as some smooth function showed that the oscillations could be reduced to an acceptable level only when the source was turned on so gradually as to noticeably increase the time required to set up a critical level. As an alternative, we introduced the linear wings on the zonal flow profile (Fig. 8) so that Rossby waves excited by the source and traveling toward the west at the speed of normal modes in the domain  $-15 \leq y^* \leq 15$  would see critical levels. Since an incident wave is absorbed at a critical level at either end of the domain, no normal mode can be set up.

A well-known restriction on the Matsuno time differencing scheme (see Matsuno, 1966) is that  $\Delta t$  must be chosen such that  $\Delta t < (1/\omega_1)$ , where  $\omega_1$  is the highest frequency normal mode of the system, whether or not that normal mode is excited by the forcing in the problem. If this condition is not met, the normal mode

is amplified without limit and the solution blows up. We noticed that the introduction of the linear wings of negative  $U$  to filter out normal modes as described above also forced a choice of smaller  $\Delta t$ . The explanation seems to be as follows. First we note that the lowest frequency normal mode in the domain, because of its large north-south scale, satisfies approximately a (dimensionless) dispersion relation of the form

$$\omega_1^* = - \left[ -U^* + \frac{\beta^*}{k^{*2} + (\pi^2/L^{*2})} \right] k^*, \quad (\text{A1})$$

where  $L^*$  is the width of the domain (30 units). Here  $U^*$  and  $\beta^*$  are to be regarded as having been averaged across the domain. In the absence of the wings,  $U^*$  is already negative (see Fig. 8) and when the wings are added it becomes more negative, increasing  $\omega_1^*$  and forcing the choice of a smaller  $\Delta t$ . We suspect, furthermore, this normal mode is not screened from the walls by critical layer absorption in the wings because its north-south scale is so large that there is little attenuation in the region between critical level and wall.

It was also found that a smaller time step must be chosen for treating lower zonal wavenumber disturbances. This can be understood from Eq. (A1). Typically  $k^* \approx O(1)$  for zonal wavenumber 5 and  $U^*$  and  $\beta^*$  are  $O(1)$  so that  $\omega_1^*$  is  $O(1)$ . For zonal wavenumber 1, on the other hand, we have

$$\omega_1^* \approx \frac{\beta^*}{k^*} \approx 5, \quad (\text{A2})$$

that is, the frequency of the lowest order normal mode is substantially higher.

#### REFERENCES

- Bennett, J. R., and J. A. Young, 1971: The influence of latitudinal wind shear upon large-scale wave propagation into the tropics. *Mon. Wea. Rev.*, **99**, 202-214.
- Charney, J. G., 1963: A note on large-scale motion in the tropics. *J. Atmos. Sci.*, **20**, 607-609.
- , 1969: A further note on large-scale motion in the tropics. *J. Atmos. Sci.*, **26**, 182-185.
- Dickinson, R. E., 1968: Planetary waves propagating vertically through weak westerly wind wave guides. *J. Atmos. Sci.*, **25**, 984-1002.
- , 1970: Development of a Rossby wave critical level. *J. Atmos. Sci.*, **27**, 627-633.
- , 1971: Analytic model for zonal winds in the tropics, 1. Details of the model and simulation of gross features of the zonal mean troposphere. *Mon. Wea. Rev.*, **99**, 501-510.
- , and F. Clare, 1973: Numerical study of the unstable modes of a hyperbolic-tangent barotropic shear flow. *J. Atmos. Sci.*, **30**, 1035-1049.
- Jones, W. L., and D. Houghton, 1971: The coupling of momentum between internal gravity waves and mean flow: A numerical study. *J. Atmos. Sci.*, **28**, 604-608.
- Krishnamurti, T. N., 1971: Observational study of the tropical upper tropospheric motion field during the Northern Hemisphere summer. *J. Appl. Meteor.*, **10**, 1066-1096.
- Mak, M., 1969: Laterally driven stochastic motions in the tropics. *J. Atmos. Sci.*, **26**, 41-64.
- Matsuno, T., 1966: Numerical integrations of the primitive equations by a simulated backward difference method. *J. Meteor. Soc. Japan*, **44**, 76-83.
- , 1971: A dynamical model of the sudden stratospheric warming. *J. Atmos. Sci.*, **28**, 1479-1494.